Tenth U.S. National Conference on Earthquake Engineering
Frontiers of Earthquake Engineering
July 21-25, 2014
Anchorage, Alaska

DEVELOPING A SOIL BRIDGE-INTERACTION MODEL FOR STUDYING THE EFFECTS OF LONG-DURATION EARTHQUAKE MOTIONS

K. T. Romney[1], A. R. Barbosa[2], and H. B. Mason[2]

ABSTRACT

The seismic response of a complete soil-bridge system subjected to shallow crustal and subduction zone earthquakes is the topic of this paper. Specifically, the effects of earthquake duration on the seismic performance of soil-bridge systems are examined. This topic is important, because many bridges worldwide are located in tectonic regions characterized by a subducting plate boundary, where high-intensity, long-duration earthquake motions are possible. To date, the effects of earthquake duration are not widely considered during seismic design of bridges. In this paper, a model of a soil-bridge system is developed in the finite element framework OpenSees. The soil-bridge system is subjected to earthquake motions of varying durations using the direct method. Comparative results show that the number of inelastic excursions in the bridge column and pile increase significantly with earthquake duration, even though other traditional measures of damage such as maximum bending moments and peak column drifts are independent of duration. The results also indicate that the number of inelastic excursions is strongly correlated with earthquake intensity measures that incorporate earthquake duration, such as significant duration and cumulative absolute velocity. The results imply that earthquake duration needs to be considered when designing and retrofitting bridge superstructures, especially when the bridge superstructures are designed to fail in flexure.

[1]Staff Engineer, Parsons Brinckerhoff, 400 SW 6th Avenue #802, Portland, OR 97204; formerly, Graduate Student Researcher, School of Civil and Construction Engineering, Oregon State University, Corvallis, OR 97331
[2]Assistant Professor, School of Civil and Construction Engineering, Oregon State University, Corvallis, OR 97331

Romney KT, Barbosa AR, Mason HB. Developing a soil-bridge interaction model for studying the effects of long-duration earthquake motions. *Proceedings of the 10th National Conference in Earthquake Engineering*, Earthquake Engineering Research Institute, Anchorage, AK, 2014.

Tenth U.S. National Conference on Earthquake Engineering
Frontiers of Earthquake Engineering
July 21-25, 2014
Anchorage, Alaska

Developing a Soil-bridge Interaction Model for Studying the Effects of Long-duration Earthquake Motions

K. T. Romney[1], A. R. Barbosa[2], and H. B. Mason[2]

ABSTRACT

The seismic response of a complete soil-bridge system subjected to shallow crustal and subduction zone earthquakes is the topic of this paper. Specifically, the effects of earthquake duration on the seismic performance of soil-bridge systems are examined. This topic is important, because many bridges worldwide are located in tectonic regions characterized by a subducting plate boundary, where high-intensity, long-duration earthquake motions are possible. To date, the effects of earthquake duration are not widely considered during seismic design of bridges. In this paper, a model of a soil-bridge system is developed in the finite element framework OpenSees. The soil-bridge system is subjected to earthquake motions of varying durations using the direct method. Comparative results show that the number of inelastic excursions in the bridge column and pile increase significantly with earthquake duration, even though other traditional measures of damage such as maximum bending moments and peak column drifts are independent of duration. The results also indicate that the number of inelastic excursions is strongly correlated with earthquake intensity measures that incorporate earthquake duration, such as significant duration and cumulative absolute velocity. The results imply that earthquake duration needs to be considered when designing and retrofitting bridge superstructures, especially when the bridge superstructures are designed to fail in flexure.

Introduction

Recent earthquakes in Chile and Japan have shown the destructive power of subduction zone earthquakes. Subduction zone earthquake motions, when compared to shallow crustal earthquake motions, typically have longer durations, higher intensities, and higher frequency contents in the low frequency (long period) range. Notably, recent subduction zone earthquakes in Chile and Japan occurred offshore; therefore, for civil structures located onshore, the source-to-site distance was larger for these subduction zone earthquakes than for typical shallow crustal earthquakes. Accordingly, earthquake intensity measures correlated to amplitude, e.g., peak ground acceleration, PGA, or the spectral acceleration at a fundamental period of the bridge-soil system, $S_a(T_1)$, can be very similar at a given site regardless of the earthquake's tectonic origin.

Transportation systems serve as lifelines in the aftermath of disastrous earthquakes. Within transportation systems, bridges are key components of a functional system. Accordingly,

[1]Staff Engineer, Parsons Brinckerhoff, 400 SW 6th Avenue #802, Portland, OR 97204; formerly, Graduate Student Researcher, School of Civil and Construction Engineering, Oregon State University, Corvallis, OR 97331
[2] Assistant Professor, School of Civil and Construction Engineering, Oregon State University, Corvallis, OR 97331

Romney KT, Barbosa AR, Mason HB. Developing a soil-bridge interaction model for studying the effects of long-duration earthquake motions. *Proceedings of the 10th National Conference in Earthquake Engineering*, Earthquake Engineering Research Institute, Anchorage, AK, 2014.

the seismic resiliency of bridges is an important topic of investigation for earthquake engineers. To this end, a two-dimensional finite element model of a soil-bridge system was developed to evaluate the effects of earthquake motions from shallow crustal and subduction zone sources on the seismic response of bridges. Within the developed model, soil-bridge interaction is accounted for by connecting the soil to the bridge pile with soil-interface springs. Furthermore, the direct method [1] for analyzing soil-bridge interaction was employed. A thorough literature review is outside the scope of this study. Readers can consult Barbosa et al. [2] for more information about soil-bridge interaction. The works by Khosravifar [3], Chiaramonte et al. [4], Zhang et al. [5], Shamsabadi et al. [6], Chang [7], Brandenberg et al. [8] and Boulanger et al. [9] were instrumental for creating the soil-bridge models and informing the research work.

Methodology

A two-dimensional (2-D) finite element model of a double-span reinforced concrete bridge and foundation connected to a nonlinear soil column by nonlinear soil springs was developed using the Open System for Earthquake Engineering Simulations (OpenSees) finite element framework [10]. The seismic response of the soil-bridge system was analyzed by subjecting the model to seven shallow crustal earthquake motions and seven subduction zone earthquake motions. Figure 1 shows a schematic of the overall soil-bridge system and a cross-section of the modeled pile and bridge column. Barbosa et al. [2] contains more details about the soil-bridge model, though some of the modeling details have changed, which are documented herein.

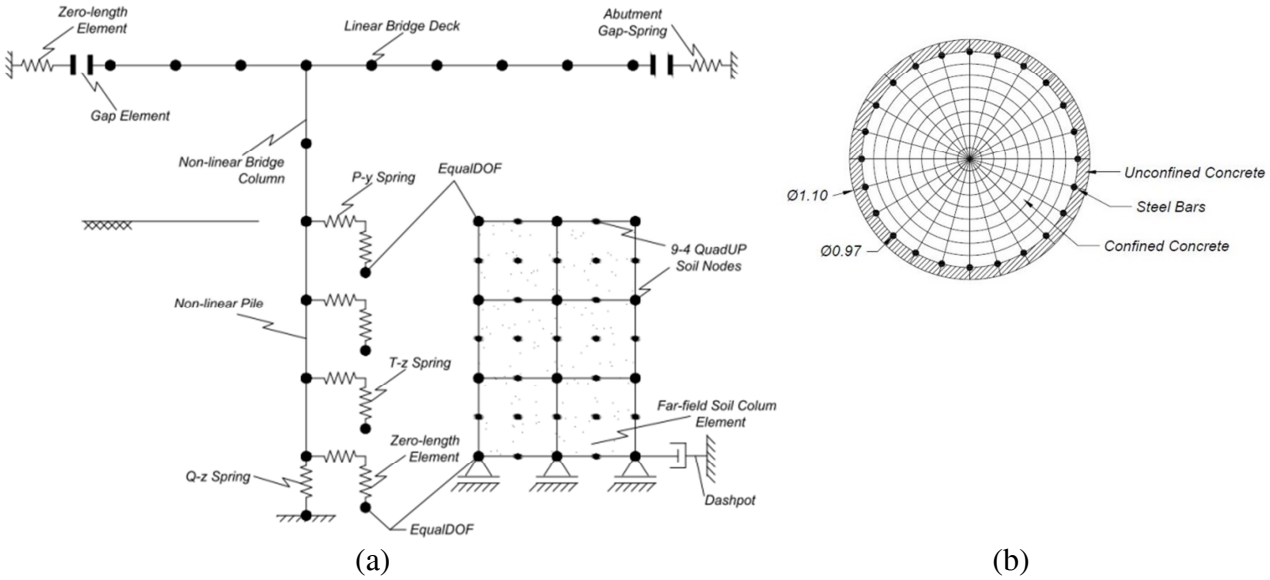

(a) (b)

Figure 1. (a) Soil-bridge system analyzed, and (b) cross-section of bridge pile and column (all dimensions are in meters) [2].

Earthquake Motion Selection

In the United States, the Pacific Northwest (PNW) and Alaska are prone to subduction zone earthquakes. Traditionally, bridges have been designed to withstand shallow crustal earthquakes, because these bridges are predominant in California. However, the subduction zone earthquake

motions have a longer duration, sometimes have a larger amplitude (depending on source-to-site distance), and often have a lower frequency content (longer period) when compared to shallow crustal earthquake motions. Accordingly, earthquake motions produced by subduction zone earthquakes can subject bridges to unique seismic demands.

For this study, Portland, Oregon (45.5200353° N, 122.6743645° W) was chosen as the site location for earthquake motion selection purposes. A target design spectrum was generated for the Portland, Oregon site using the AASHTO LRFD Bridge Design Specifications for soil type C based on the combined soil-bedrock shear wave velocity of the site to a depth of 30 m [11]. Subduction zone earthquake motion selection was performed using databases of earthquake recordings from the 2011 Great East Japan Earthquake [12] and the 2010 Chilean Earthquake [13]. The shallow crustal earthquake motions were selected based on magnitude, source-to-site distance, shear wave velocity, and earthquake mechanism [14]. Selected shallow crustal earthquake motions were restricted to earthquakes with moment magnitudes of $M_w = 7.0 \pm 0.5$ and source-to-site distances R = 20 to 40 km. To match the target spectrum, a linear scaling factor, *SF*, was applied to each motion. The *SF* was bounded by a factor of five, i.e., $0.2 < SF < 5.0$. A root-mean-square-error (RMSE), which measures the goodness-of-fit between the response spectrum and the target spectrum, was calculated for each *SF*. Ultimately, earthquake motions with minimum RMSE values and *SF*s closest to 1.0 were chosen for analysis.

The shallow crustal and subduction zone earthquake motions were linearly scaled to match the same target spectrum, which is an unconventional earthquake motion selection strategy. Our primary goal was to study the effect of earthquake motion duration on seismic soil-bridge performance. Therefore, the selection strategy was performed so the amplitudes and, to a lesser extent, the frequency contents of the two types of earthquake motions would be roughly similar. Details of the final selected earthquake motions are available in Barbosa et al. [2].

Soil-Foundation-Bridge Model Development

The soil is modeled with a uniform 2D soil mesh with the plain-strain assumption. The soil is atop a compliant bedrock (shear wave velocity, V_s = 760 m/s) layer. The soil-bedrock fixity is modeled with roller connections. The compliance of the bedrock is modeled with a dashpot [4]. The mesh consists of 9-4 quadrilateral u-p elements with nine Gauss integration points [15]. Nodes of the soil mesh with the same elevation are constrained to have the same displacements; i.e., the shear beam assumption was employed. Dense, homogeneous, non-liquefiable sand was used for the soil type. The Pressure-Dependent-Multi-Yield (PDMY) material model [15] was used to define the constitutive behavior of the dense sand. The constitutive soil parameters used for the PDMY model are given in Barbosa et al. [2]. The total height of the soil column was 20 m, which matches the length of the bridge pile. The width of the soil column was one meter. Barbosa et al. [2] performed a model-specific sensitivity analysis regarding out-of-plane thickness and found that choosing an out-of-plane thickness of 10 m (i.e., the width of the bridge deck) was acceptable, which complies with findings from other researchers [e.g. 5, 16]. The individual height of the soil elements was selected based on the relationship $h_{max} = V_s / (8 f_{max})$, where h_{max} is the maximum height of a soil element, f_{max} is the maximum frequency of interest, and V_s is the shear wave velocity of the softest layer (V_s = 250 m/s, for the dense sand). A soil element size of one meter was ultimately chosen to satisfactorily meet the aforementioned

criterion.

The soil-interface springs connect the pile foundations to the surrounding soil and represent the flexibility of the soil-pile interface. Three types of soil-interface springs are used to model the soil-pile interface: lateral resistance (p-y), skin friction (t-z), and end bearing resistance (q-z). The parameters defining the soil springs were chosen in accordance with recommendations from API [17]. Additionally, the p-y and t-z element stiffnesses (i.e. subgrade moduli) were modified at larger depths to account for overburden effective stress [9]. Each spring is defined by an ultimate resistance (p_{ult}, t_{ult}, and q_{ult}) and the displacement at which 50% of the ultimate resistance is mobilized (i.e. y_{50} for p-y and z_{50} for the t-z springs) [9]. A more in depth discussion of the meaning and contribution of each parameter is provided by Boulanger et al. [18]. Gapping effects are modeled after Boulanger et al. [9] by incorporating residual resistance or drag force along the sides of the pile. The drag coefficient, C_d, is defined as the ratio of the residual resistance to the ultimate resistance, p_{ult}. A value of 0.3 was used as the drag coefficient to define the drag resistance within a fully mobilized gap. The drag resistance, R_d, is calculated by multiplying the coefficient of drag by the ultimate resistance of the p-y spring [19].

The reinforced-concrete bridge pile is 6.1 m in height and 1.1 m in diameter. The bridge pile cross-section consists of a confined concrete core, an unconfined concrete cover with a specified concrete strength of 28 MPa, and 16 #10 ASTM A706 Grade 60 ksi (475 MPa) reinforcing steel bars placed at the confined and unconfined concrete interface (shown in Figure 1b). The bridge pile is modeled using the flexibility-based nonlinear beam-column element [24]. The material model used for the concrete fibers was specified based on the Yassin [20] concrete model (designated as *Concrete02* in OpenSees), which includes linear tension softening for the concrete. Two uniaxial material models were used to define the unconfined and confined concrete stress-strain response. Material parameters for the confined concrete were defined based on the Karthik and Mander [21] model. The fibers of the reinforcing steel were modeled using the Filippou et al. [22] model, which is designated in OpenSees as *Steel02*. A sensitivity of the moment-curvature response was performed by considering increasing the number of fibers in the cross-section definition of the bridge pile [2]. The sensitivity analysis revealed that a discretization of 16 radial divisions and 16 theta wedges provided sufficient accuracy without introducing significant computation costs.

The bridge superstructure consists of two 31.7 m-long spans, with a total width of 10.36 m and height of 1.67 m [6]. No inelastic response is expected from the deck, which is post-tensioned; therefore, the box girder is modeled using linear elastic beam-column elements, which are located 0.93 m above the top of the column. Rheological effects of creep and shrinkage are not considered in this model. The bridge superstructure and column are connected monolithically by a 0.93 m-long rigid elastic beam-column element was used. This rigid element was modeled by applying a factor of 1000 to the entire bridge deck stiffness (*EI*).

The bridge abutments are dimensioned in height and width to accommodate and support the bridge deck. Expansion joints are provided at either end of the deck, which are modeled in OpenSees with compressive, elasto-perfectly-plastic gap elements. For longitudinal displacements of the deck, less than the initial opening of the gap, the supports act like rollers. Under large displacements of the deck the gap provided by the expansion joint closes and the

deck pounds on the abutments. Thus, the capacity of the abutment (backwall and backfill) as well as the stiffness of the abutment system have to be defined and are only activated once the initial gap is reduced to zero. By design, the abutment backwall is assumed to shear off; thus, the peak capacity and stiffness are provided primarily by the backfill. The backfill is assumed to be a silty sand as specified by Caltrans [23] and shown in Shamsabadi et al. [6]. Using these assumptions, the gap element, as defined in OpenSees, has a stiffness, K = 307 kN/cm/m, yield force, F_y = 1397 kN (determined as specified in [23]), and initial gap opening = 2.54 cm [6].

To determine the modal parameters of the structure and the fundamental period of the soil-foundation-abutment-bridge system and mode shape, an eigenvalue analysis was performed within OpenSees, and the first fundamental period was found to be 0.89 seconds. Rayleigh damping was used to model the material damping of the soil-foundation-bridge system [24]. The baseline damping ratio, ζ, was set to 2% at frequencies of 1.12 Hz (first mode of the soil-bridge system) and 20 Hz (approximately the third mode of the soil-bridge system).

Analysis Methodology

The nonlinear FE analysis of the soil-foundation-bridge system is divided into four stages to simulate in-situ soil conditions both pre- and post-construction and to incorporate the effects of staged construction of the structural components.

- Stage 1: The geometry (nodes and connectivity) and constraints of the soil column, the bridge superstructure, and the bridge pile are defined.
- Stage 2: The linear elastic deck and non-linear pile and column element nodes and connectivity are defined. Bridge column cross-section fiber discretization is assigned. Non-linear constitutive relationships are assigned to each fiber (unconfined concrete, confined concrete and steel). The lateral, vertical, and end bearing nonlinear interface springs are created and connected to the soil column, but not to the bridge pile.
- Stage 3: The soil gravity load is applied. The pile and soil column are connected by the nonlinear soil-interface springs. Gravity loading is applied to the bridge superstructure. For the gravity loading, a transient analysis, with large numerical damping introduced to simulate critically-damped quasi-static loading, is performed to solve the equilibrium equations using the Krylov-Newton algorithm [25].
- Stage 4: The nonlinear dynamic time-history analyses are performed using the Newmark constant average acceleration method and assigning the iteration time step to of 0.005 sec. P-Δ effects are considered in the analysis.

Results

Two earthquake motions are selected to examine the seismic response of the soil-bridge system in detail: (1) the 1992 Landers Yerma Fire Station motion (shallow crustal), and (2) the 2011 Japan IWTH1111 Station motion (subduction zone). Herein, the two earthquake motions are referred to as the "Landers motion" and the "Japan motion," respectively. The peak ground accelerations (PGA) are 0.27 g and 0.33 g for the Landers motion and Japan motion, respectively, and the significant durations ($D_{5\text{-}95}$) are 18.9 sec and 102 sec for the Landers motion and Japan motion, respectively.

Figure 3 presents the peak column and pile axial load, overturning moment, shear force, and displacement for the (a) Landers and (b) Japan earthquake motions. The axial load is normalized by the design axial load, P_D = 3483 kN, the overturning moment is normalized by the moment at first yield, M'_y = 2720 kN-m, and the shear force is normalized by the seismic weight, W_S = 7180 kN. The seismic weight was taken as the weight of the structure above the ground surface. The displacement is presented as peak horizontal displacement in the column and soil, which are normalized by the maximum displacement of the column. Each parameter is plotted against the depth normalized by the column/pile diameter.

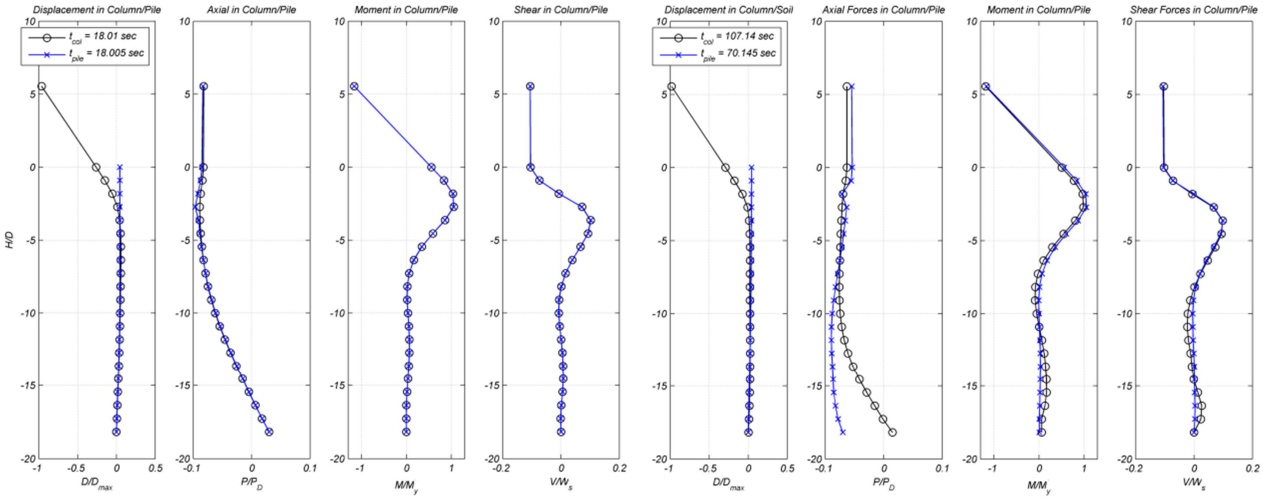

(a) (b)

Figure 3. Column Forces at peak overturning moment in pile and at the top of the column due to (a) Landers and (b) Japan earthquake motion. The displacements of the soil (denoted by pile subscript) and column are presented in the first figure whereas the other three figures present the forces in the column and pile.

When the soil-bridge system was subjected to the Landers earthquake motion, the peak axial force, overturning moment, and shear force in the column and pile exceeded the corresponding quantities caused by the Japan earthquake motion. The maximum bending moment in the pile during the Japan earthquake motion approaches the first yielding moment, M'_y. The maximum bending moment in the pile exceeds the yield moment during the Landers motion and also during the Japan motion. The tensile capacity of the confined and unconfined concrete was exceeded during both motions. The compressive strength of the unconfined concrete cover reaches 100% of its resistance; therefore, the bridge column is expected to experience spalling of the cover during both motions shortly after strong shaking begins (for concrete compressive strains greater than 0.004 m/m). The ability to resist the dynamic loading is decreased, especially during the Landers motion, after 100% of the compressive strength is reached.

Figure 4 shows the number of inelastic excursions with respect to the effective plastic hinge rotation, θ_{lp}, which is computed by $\theta_{lp} = \phi L_p$, where ϕ is the curvature and L_p is the

effective plastic hinge length [26]. The yield rotation, θ_Y, corresponds to the curvature at the point of first yield, ϕ_Y, of the moment-curvature analysis multiplied by the effective plastic hinge length, L_p. The number of inelastic excursions is defined as the number of peaks exceeding the yield rotation, θ_Y. Table 1 reports the mean, median, standard deviation, and coefficient of variation of the number of inelastic excursions for crustal and subduction zone earthquake motions. The mean and median numbers of inelastic excursions for the subduction zone earthquake motions are 5 and 6 times greater than for the shallow crustal earthquake motions, respectively. The standard deviation shows an increase in scatter for the subduction zone earthquake motions compared to that of the shallow crustal earthquake motions. It is worth noting that the large coefficients-of-variation observed indicate that a larger number of records should be used to check if the dispersion in the results can be reduced, but it is part explained by the variability in duration of the motions from Chile and Japan.

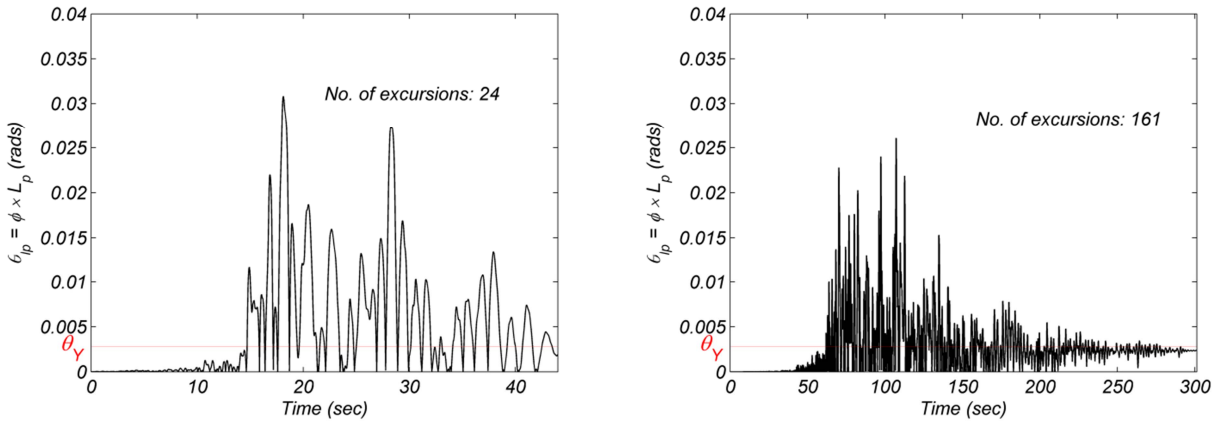

Figure 4. Effective plastic hinge rotation, θ_{lp}, for the (a) Landers and (b) Japan earthquake motions. The yield rotation, θ_Y, corresponds to the curvature at the point of first yield, ϕ_Y, of the moment-curvature analysis multiplied by the effective plastic hinge length.

Figure 5a and 5b illustrates the correlogram of the number of inelastic excursions versus $S_a(T_1)$ and D_{5-95} for both shallow crustal earthquake motions and subduction zone earthquake motions, respectively. $S_a(T_1)$, which does not incorporate the effects of earthquake motion duration, shows a very low correlation; contrastingly, the significant duration, which does incorporate the effects of earthquake motion duration, shows a roughly linear trend. The majority of the subduction zone earthquake motions plot in the upper right-hand corner, and the shallow crustal earthquake motions plot much closer to the origin. It should be noted, that even though this clear trend is observed, a larger number of earthquake ground motions should be employed before reaching statistically meaningful results.

Conclusions

The primary goal of this work was to develop an understanding of the effects of duration on the seismic response of a soil-foundation-bridge system. A suite of fourteen earthquake motions was selected; seven shallow crustal and seven subduction zone. The earthquake motions were

amplitude scaled so that their amplitudes were similar, and they were selected to have similar spectral shape (frequency content); thus, the distinguishing factor between the two types of earthquake motions was the duration. The subduction zone earthquake motions used had longer durations, as is typical, and this means that they had more inelastic cycles of vibration.

Table 1. Summary table of the mean, median, standard deviation (SD), and coefficient of variation (COV) of the number of inelastic excursions for both shallow crustal and subduction zone earthquake motions

Earthquake Type	Mean	Median	SD	COV
Shallow crustal	23.9	24.0	4.88	0.205
Subduction	123	141	57.9	0.471

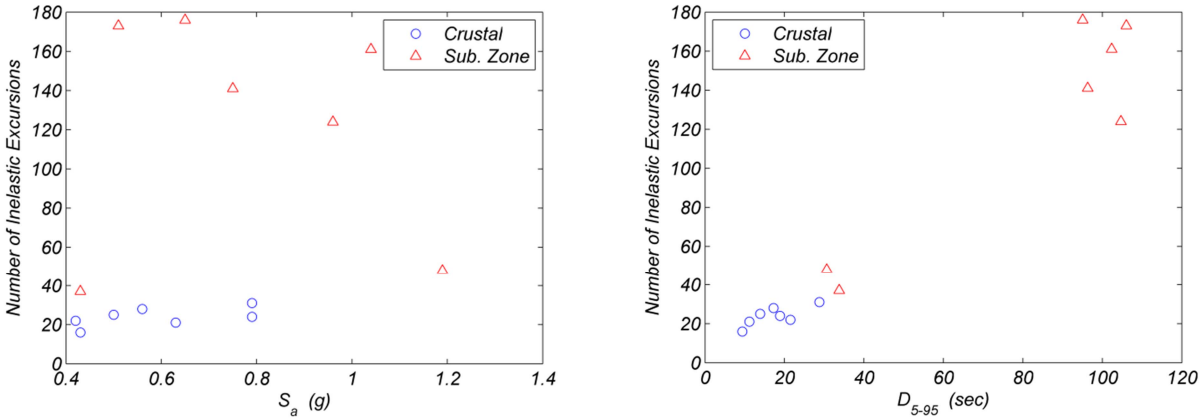

(a) (b)

Figure 5. (a) Spectral acceleration and (b) significant duration ($D_{5\text{-}95}$) for all earthquake motions relating to number of inelastic excursions

Examining the results, it was found that the displacement, shear force, and bending moment versus depth profiles were similar when shallow crustal or subduction zone earthquake motions were considered. In addition, the plastic hinging in the bridge column/pile occurred at nearly the same location and, in some cases, extent of plastic hinging was worse for the shallow crustal earthquake motions than the subduction zone earthquake motions. The drifts, shear forces, and bending moments were not as sensitive to duration, when peak values were being examined.

When the number of inelastic excursions was examined, the effects of duration became apparent. The number of inelastic excursions recorded during the subduction zone earthquake motions was approximately four times greater than the number of inelastic excursions recorded during the shallow crustal earthquake motions. This indicates that damage in the bridge columns, primarily due to low-cycle and extremely low-cycle fatigue, is expected to be much greater during the subduction zone earthquake motions. Low-cycle and extremely low-cycle fatigue are critical modes of failure in columns designed to current codes, when the columns are designed to fail in flexure.

The number of inelastic excursions was compared to earthquake motion intensity measures to start framing this problem within the performance-based earthquake engineering (PBEE) framework [27]. The earthquake motion intensity measures examined are peak ground acceleration (PGA), the spectral acceleration at the fundamental period of the soil-foundation-bridge system [$S_a(T_1)$], and the significant duration (D_{5-95}). It was found that PGA and $S_a(T_1)$ were poor indicators of the expected number of inelastic excursions caused by an earthquake motion, which is expected, because the ground motions were selected to have similar spectral shapes. D_{5-95} is a much better indicator of the number of inelastic excursions, which is expected, because D_{5-95} includes the effects of earthquake motion duration explicitly. Fourteen earthquake motions are not sufficient for drawing statistically significant distinctions regarding the sufficiency and efficiency of the chosen earthquake motion intensity measures for predicting the number of inelastic excursions. This will be the topic of a much larger future research program, as this work moves closer to completing the PBEE analysis, and finally predicting expected losses caused by subduction zone earthquake motions.

Acknowledgments

The Region 10 University Transportation Center, referred to as PacTrans, supported the work presented in this paper. The authors gratefully acknowledge the advice given by Pedro Arduino (University of Washington) regarding some details of soil-structure interaction modeling in OpenSees, and the thorough review by Joe Wang (Parson Brinkerhoff).

References

1. Kramer SL, Stewart JP. Geotechnical aspects of seismic hazards. In *Earthquake Engineering from Engineering Seismology to Performance Based Engineering*. Bozorgina Y, Bertero, VV (eds). CRC Press: Boca Raton, FL, 2004.
2. Barbosa AR, Mason HB, Romney K. "SSI-Bridge: Solid-Bridge Interaction During Long-Duration Earthquake Motions," University of Washington, Seattle, WA, USDOT University Transportation Center for Federal Region 10, PacTrans Report, 2014.
3. Khosravifar A. Analysis and design for inelastic structural response of extended pile shaft foundations in laterally spreading ground earthquakes. *PhD Thesis*, University of California, Davis, California, 2012.
4. Chiaramonte MM, Arduino P, Lehman D, Roeder C. Seismic analyses of conventional and improved marginal wharves. *Earthquake Engineering and Structural Dynamics* 2013, **42(10)**: 1435-1450.
5. Zhang Y, Conte JP, Yang Z, Elgamal A, Bielak J, Acero G. Two-dimensional nonlinear earthquake response analysis of a bridge-foundation-ground system. *Earthquake Spectra* 2008, **24(2)**: 343–386.
6. Shamsabadi A, Rollins KM, Kapuskar M. Nonlinear soil–abutment–bridge structure interaction for seismic performance-based design. *Journal of Geotechnical and Geoenvironmental Engineering* 2007, **133(6)**: 707–720.
7. Chang D. Inertial and lateral spreading demands on soil-pile-structure systems in liquefied and laterally spreading ground during earthquakes. *PhD Thesis*, University of California, Davis, California 2007.
8. Brandenberg SJ, Boulanger RW, Kutter BL, Chang D. Behavior of pile foundations in laterally spreading ground during centrifuge tests. *Journal of Geotechnical and Geoenvironmental Engineering* 2005, **131(11)**: 1378–1391.
9. Boulanger RW, Curras CJ, Kutter BL, Wilson DW, Abghari A. Seismic soil-pile-structure interaction experiments and analyses. *Journal of Geotechnical and Geoenvironmental Engineering* 1999, **125(9)**: 750–759.

10. McKenna F, Scott MH, Fenves GL. Nonlinear finite element analysis software architecture using object composition. *Journal of Computing in Civil Engineering* 2010, **24(1)**: 95-107.
11. AASHTO, LRFD. *Bridge Design Specifications*. American Association of State Highway and Transportation Officials: Washington, DC, 2012.
12. National Research Institute for Earth Science and Disaster Prevention. *Strong-motion seismograph networks* http://www.k-net.bosai.go.jp/ (accessed Feb. 2013).
13. Boroschek RL, Contreras V, Kwak DY, Stewart JP. Strong ground motion attributes of the 2010 Mw 8.8 Maule, Chile, earthquake. *Earthquake Spectra* 2012, **28(1)**: 19–38.
14. Baker JW, Lin T, Shahi SK, Jayaram N. New ground motion selection procedures and selected motions for the PEER transportation research program. *PEER-2011/03.* Pacific Earthquake Engineering Research Center: Berkeley, California, 2011.
15. Elgamal A, Yang Z, Parra E. Computational modeling of cyclic mobility and post-liquefaction site response. *Soil Dynamics and Earthquake Engineering* 2002, **22(4)**: 259–271.
16. Chang D, Boulanger R, Brandenberg S, Kutter B. FEM analysis of dynamic soil-pile-structure interaction in liquefied and laterally spreading ground. *Earthquake Spectra* 2013, **29(3)**: 733-755.
17. American Petroleum Institute (API). *Recommended Practice for Planning, Designing and Construction Fixed Offshore Platforms*. American Petroleum Institute: Washington, D.C., 1993.
18. Boulanger RW, Kutter BL, Brandenberg SJ, Singh P, Chang D. Pile foundations in liquefied and laterally spreading ground during earthquakes: Centrifuge experiments & analyses. *Report No. UCD/CGM-03/01*. University of California, Davis, California, 2003.
19. Spacone E, Filippou FC, Taucer FF. Fiber beam-column model for non-linear analysis of R/C frames: Part I. Formulation. *Earthquake Engineering and Structural Dynamics* 1996, **25(7)**: 711-726.
20. Yassin MHM. Nonlinear Analysis of Prestressed Concrete Structures under Monotonic and Cycling Loads. *PhD Thesis*, University of California, Berkeley, California, 1994.
21. Karthik MM, Mander JB. Stress-block parameters for unconfined and confined concrete based on a unified stress-strain model. *Journal of Structural Engineering* 2010, **137(2)**: 270–273.
22. Filippou FC, Bertero VV, Popov EP. *Effects of bond deterioration on hysteretic behavior of reinforced concrete joints*. Earthquake Engineering Research Center: Berkeley, California, 1983.
23. California Department of Transportation. *Seismic Design Criteria*, Sacramento, California, 2006.
24. Chopra AK. *Dynamics of structures: Theory and applications to earthquake engineering, Volume 4*. Prentice Hall Saddle River: New York, New York, 2012.
25. Scott MH, Fenves GL. Krylov subspace accelerated newton algorithm: application to dynamic progressive collapse simulation of frames. *Journal of Structural Engineering* 2009, **136(5)**: 473–480.
26. Priestley MJN, Seible F, Calvi GM. *Seismic Design and Retrofit of Bridges*. John Wiley and Sons, Inc: New York, New York, 1996.
27. Kramer SL. Performance-based design in geotechnical earthquake engineering practice. In *Fifth International Conference on Earthquake Geotechnical Engineering*, Santiago, Chile, 2011.